

# Room Temperature Tryptophan Phosphorescence of Proteins in the Composition of Biological Membranes and Solutions

Vladimir M. Mazhul', Alexander V. Timoshenko, Ekaterina M. Zaitseva, Svetlana G. Loznikova, Inessa V. Halets, and Tatsiana S. Chernovets

**Abstract** The room temperature tryptophan phosphorescence (RTTP) technique allows studying slow internal dynamics of proteins in the millisecond and second diapasons. This chapter summarizes the key findings in the field of RTTP spectroscopy, physical nature of this phenomenon, and experimental approaches to analyze the microenvironment of tryptophan residues. Representative examples of RTTP of proteins in human erythrocyte membranes and plant lectins in solutions are discussed in details taking into account the effects of detergents on biological membranes and 3D structures of lectin molecules, respectively.

## 1 Introduction

The regulation of almost all processes occurring in the biosphere at the molecular level is related to the functioning of proteins. The functional activity of proteins is determined in many respects by their structure – the conformation and the internal dynamics. Spectroscopic methods based on a registration of the spectral, temporal, and polarization parameters of the fluorescence of tryptophan residues [1–3] are widely used in the investigation of the structure of proteins. However, the most suitable means for the study of the internal dynamics of proteins is provided by the room temperature tryptophan phosphorescence (RTTP). As compared to the fluorescence, the RTTP monitors much slower processes, extending the observation time from the nanosecond range of fluorescence up to millisecond to second range of phosphorescence.

The RTTP spectra of proteins in the condensed state were detected for the first time in 1966 [4]. The RTTP of proteins in solution was first described in 1974 [5]. The RTTP spectra and decay kinetics of two globular proteins – horse-liver alcohol dehydrogenase and *Escherichia coli* alkaline phosphatase – were measured in

---

V.M. Mazhul' (✉)

Laboratory of Proteomics, Institute of Biophysics and Cellular Engineering, National Academy of Sciences of Belarus, 27 Akademicheskaya Str., Minsk, 220072, Belarus  
e-mail: mazhul@biobel.bas-net.by

oxygen-pured solution. The RTTP lifetime ( $\tau$ ) of proteins was found to be sensitive to changes in pH and solvent viscosity, to the action of guanidine hydrochloride (1 M) and ligand binding. It was suggested that the efficiency of quenching of RTTP depends on the fluctuations in the structure of the protein. In 1976, the spectra and RTTP decay kinetics of the suspensions of isolated human erythrocyte membranes, chick embryo fibroblasts, and yeast microorganisms *Candida utilis* were described [6]. It was established that RTTP decay of isolated membranes and fibroblasts changes under the action of noradrenalin ( $10^{-4}$  M) and calcium cations ( $10^{-2}$  M). In that work the capability of horse-liver alcohol dehydrogenase in solution to exhibit RTTP was confirmed. The spectra and RTTP decay of a solution of rabbit muscle aldolase were recorded for the first time. It was shown that denaturation of rabbit muscle aldolase under the action of urea (4–6 M) or heat leads to a dramatic decrease in the lifetime and total phosphorescence intensity.

In following years it was demonstrated that RTTP spectroscopy is exquisitely sensitive to slow internal dynamics of the protein structure in the vicinity of tryptophan residues. It has been shown that changes in the RTTP lifetime reflect changes in the local rigidity of protein structure and the phosphorescence lifetime can be used as an intrinsic monitor of local flexibility of protein structure in regions of localization of tryptophan residues in the millisecond and second range. The dominating quenching mechanism of tryptophan phosphorescence in the oxygen-pured medium is deactivation of triplet excited states due to collisions of the indole ring of a tryptophan residue with the surrounding structural elements of the globule. The frequency of these collisions resulting in out-of-plane vibrations of the indole ring and relaxation of triplet states defines the efficiency of dynamic quenching of the tryptophan phosphorescence. The tryptophan residues located in protein regions with high dense packing of atoms characterized by rigid structure show long-lived phosphorescence at room temperature with  $\tau$  ranging from several seconds to hundreds of milliseconds. As a rule such regions of protein are disposed in rigid hydrophobic core of globule. The RTTP lifetime of residues located in more mobile environments is reduced to the values from several tens of milliseconds to several milliseconds. The triplet excited states of tryptophan residues located in the nonstructured regions at the periphery of the globule with a low dense packing of atoms (in the highly mobile environment) are deactivated mainly via a nonradiative mechanism, resulting in the effective dynamic quenching of RTTP. In this case, the RTTP lifetime decreases to 1–0.5 ms. Since the quantum yield of the RTTP of such residues is very low (lower than  $10^{-7}$ ), a phosphorescence signal from it could not always be detected [7–24]. Thus, monitoring of the slow internal dynamics of proteins in the millisecond and second range with the use of RTTP spectroscopy is possible due to the high sensitivity of the lifetime of the tryptophan phosphorescence to the mobility of the chromophore microenvironment and the correspondence of the values of lifetimes of RTTP to the characteristic times of low-frequency structural fluctuations of macromolecule.

Along with the dynamic quenching of the tryptophan phosphorescence, static quenching takes place when the indole ring of a tryptophan residue is in close contact with the phosphorescence quenching amino acid residue(s)

(intramolecular quenching). Such amino acids can be divided into three classes by their ability to quench tryptophan phosphorescence: (1) strongly quenching ( $k_q \approx 5 \times 10^8 \text{ M}^{-1} \text{ s}^{-1}$ ), such as cystine and cysteine; (2) intermediate quenching ( $k_q \approx 5 \times 10^5 - 2 \times 10^7 \text{ M}^{-1} \text{ s}^{-1}$ ), such as tyrosine, histidine, and tryptophan; (3) weakly quenching or nonquenching ( $k_q \leq 10^5 \text{ M}^{-1} \text{ s}^{-1}$ ), all other amino acid residues [16]. A special role is played by disulfide groups in the intramolecular quenching. Their pronounced ability to quench RTTP is due to their capability to accept electrons from tryptophan in the triplet excited state [18]. Static quenching of the RTTP by amino acids occurs when the distance between the indole ring and the quenching group does not exceed several angstroms. Besides distance, phosphorescence quenching efficiency depends substantially on the orientation of the quenching group relative to the indole ring of a tryptophan residue. Intramolecular quenching may occur not only if the indole ring is in permanent contact with the quenching amino acid residue but also if it is transiently brought into contact with the quencher by fluctuations in the structure of the protein. Since the distance between the indole ring and the quencher as well as their mutual orientation can periodically change with fluctuations in the molecular structure, the internal dynamics of the protein can influence the efficiency of the intramolecular quenching of the RTTP [16]. Therefore, the presence of the potential RTTP quenching residues in the tryptophan residue microenvironment does not necessarily result in phosphorescence quenching. Because of the difficulty in taking into account all factors causing the triplet excited state deactivation, it is not always possible to define precisely the phosphorescence parameters of individual tryptophan residues in multitryptophan proteins.

The phosphorescence method based on RTTP lifetime measurements was used for the studies of changes in the flexibility of the proteins in solution induced by denaturation and renaturation [5, 6, 21, 25–31], transition of the protein conformations into partially folded states [21, 27, 32–36], upon changes in the solvent viscosity [5, 21, 37, 38], hydrostatic pressure [39], pH and ionic strength [5, 15, 21, 40–43], binding of substrates, inhibitors, or allosteric effectors [5, 11, 21, 26, 44–49], removal of metal cations from the active center of an enzyme [21, 26, 50], limited proteolysis [21, 51], and association and aggregation [11, 21, 46, 47].

The RTTP of proteins in biological membranes and cells has been investigated to a much lesser extent as compared to the proteins in solution. In one of the few studies of the RTTP of cells [52], the phosphorescence properties of suspensions of *E. coli* strains containing varying amounts of alkaline phosphatase (the protein with a large quantum yield and RTTP lifetime) were investigated. It was shown that only *E. coli* alkaline phosphatase-rich strain exhibits long-lived RTTP. RTTP lifetime of *E. coli* mutant, which had no alkaline phosphatase, was less than 5 ms. The ability of suspensions of *E. coli* strains containing varying amounts of alkaline phosphatase to exhibit RTTP was re-examined in work [53]. On the basis of the data obtained it was concluded that all *E. coli* strains, independent of the amount of alkaline phosphatase, exhibit long-lived RTTP. Intensity and RTTP lifetime of *E. coli* alkaline phosphatase-rich strain were found to be much higher than that of the bacteria containing a usual amount of alkaline phosphatase or free of it. RTTP decay

of suspensions of *E. coli* alkaline phosphatase-rich strain was single exponential with a lifetime of about 2 s, i.e., it was analogous to the decay time of the RTTP of purified alkaline phosphatase in solution. Long-lived RTTP decay kinetics of suspensions of the *E. coli* strains, containing a usual amount of alkaline phosphatase or free of it, has been satisfactorily approximated by a sum of two components. It is most probable that the authors of [52] failed to detect the long-lived RTTP of *E. coli* strains with low content (usual for the *E. coli* cells) of alkaline phosphatase because its phosphorescence intensity was below the detection limits of their apparatus.

Unlike the proteins in fluid solution, all samples of the isolated biological membranes, uncolored microorganisms, plant and animal cells showed a reliably detectable long-lived RTTP. Their RTTP spectra have maxima at 410–415, 440–449, and 465–470 nm, respectively. The decay kinetics of RTTP of isolated membranes and cells was adequately approximated by the sum of two exponentials with varying lifetimes and contributions of the components. Since the majority of proteins in solution are incapable of exhibiting long-lived RTTP [9, 12, 14, 21], the question of possible source of phosphorescence signals of cells has been raised. In order to elucidate this question the comparative analysis of the capability of the membrane proteins in situ and water-soluble proteins of animal cells (rat hepatocytes) and microorganisms (bacteria *E. coli*) has been carried out [9, 53, 54]. It has been shown that long-lived RTTP of cells is determined by proteins in the composition of membrane structures. The RTTP lifetimes of the most soluble proteins of animal and bacterial cells were two or three orders smaller than those of the membrane proteins in situ. By using the example of the *E. coli* mutant strain containing an anomalously large amount of alkaline phosphatase, it was shown that the soluble proteins can contribute significantly to a phosphorescence signal of a cell only in relatively rare cases where these proteins have a high RTTP quantum yield and are present in the cell in large quantities [53]. The existence of the dramatic differences in the capability to exhibit long-lived RTTP between the membrane proteins in situ and water-soluble proteins of a cell provides a unique possibility of a selective investigation of the internal dynamics of living cell membrane proteins in situ.

Changes in the RTTP decay kinetics of cell culture of the rat pheochromocytoma PC12 under the action of the epidermal growth factor and the neuronal growth factor in physiological concentrations ( $10^{-8}$ – $10^{-12}$  M) [54, 55], the *C. utilis* microorganisms experiencing intercellular contact interactions [21], transformed into the anabiosis and reactivation states [21], under the action of biologically active substances of the humic nature [56] and ethanol [21], Chinese hamster fibroblasts subjected to an oxidation stress [57], human platelets after the treatment with trypsin at low concentrations [58–60], human peripheral blood lymphocytes, induced by binding of the HLA antibodies [61], and lectin concanavalin A at mitogenic concentrations (3  $\mu$ g/ml) [54] were reported. These results are the evidence of changes in the slow internal dynamics of membrane proteins in situ. Changes in RTTP lifetimes of cells at the pathology made it possible to use the RTTP method for the diagnosis of autoimmune diseases and cancer [21, 62].

The RTTP of uncolored plant cells was detected. Their RTTP spectra were recorded and the decay kinetics was monitored. Differences in the RTTP kinetic

parameters of plant cells for diverse species and varieties have been discovered [21, 63, 64]. It has been established that the decay kinetics of RTTP of plant cells changes under the action of brassinosteroid hormones at physiological concentrations ( $10^{-8}$ – $10^{-12}$  M) [63].

Despite a certain progress toward an understanding of the RTTP of biological membranes and cells, many problems still remain to be solved. In particular, the reasons for the dramatic differences in the capability to exhibit RTTP between the majority of proteins in solution and the proteins in the composition of biological membranes are not clearly understood. The question of differences in the capability of integral and peripheral membrane proteins to exhibit RTTP has not been investigated experimentally. Little is known about how the protein–protein and protein–lipid interactions influence the parameters of the RTTP of membrane proteins. Investigations to be carried out in the indicated directions will allow to clarify the poorly studied problem on the internal dynamics of membrane proteins. In Sect. 2, results of phosphorescence analysis of isolated membranes of human erythrocytes are presented. These data contribute to the solution to these problems.

Phosphorescence measurements of deoxygenated samples (residual oxygen concentration did not exceed 1 nM) were carried out with the conventional home-made instruments, described elsewhere [54, 65, 66]. A shutter arrangement permitted the delayed emission to be detected 1 ms after the excitation cutoff. RTTP decay kinetics was analyzed in terms of a sum of exponential components by a non-linear least square fitting using Origin 8.0 software (Microcal Software, USA). All decay data reported here are averages obtained from three or more independent measurements. Spectra were not corrected for instrumental response.

## **2 Room Temperature Tryptophan Phosphorescence of Proteins of Isolated Human Erythrocyte Membranes**

Isolated membranes of human erythrocytes represent a convenient investigation object that is frequently used in the membranology. This is explained by the fact that preparations of isolated membranes can be easily obtained and they are homogeneous, i.e., free of impurities of cellular organelle membranes. Moreover, the erythrocyte membranes are organized by the principles that are common for all the biological membranes. The membrane of a human erythrocyte is heterogeneous in composition and in structural organization of the proteins embedded in it. Integral proteins, also called transmembrane proteins, span the lipid bilayer and typically contain one or more hydrophobic transmembrane helices. Integral proteins of erythrocyte membrane are represented by band 3, glycophorins, different ATPases ( $K^{+}$ – $Na^{+}$ -ATPase,  $Mg^{2+}$ -ATPase,  $Na^{+}$ -ATPase, and  $Ca^{2+}$ -ATPase). A major membrane-spanning integral protein is band 3. Peripheral proteins are layered on the surface of a plasma membrane. Spectrin (bands 1 and 2), actin (band 5), ankyrins (bands 2.1–2.3), proteins of bands 4.1, 4.2, and glyceraldehyde 3-phosphate dehydrogenase (band 6) belong to this class of proteins. Spectrin and

actin comprise about 30% of all of the proteins contained in the plasma membrane of an erythrocyte. These proteins organize spectrin–actin network, representing the base of the cytoskeleton, on the cytoplasmic side of the membrane. The ankyrins play an important role in the stabilization of the cytoskeleton structure. Spectrin is associated with integral membrane proteins by attachment to ankyrin. The protein of band 4.1 with adducin promotes spectrin–actin interaction and forms a ternary complex with the transmembrane protein glycophorin C and the membrane-associated guanylate kinase p55. The protein of band 4.2 interacts with cytoplasmic domain of the anion exchanger (band 3), ankyrin, spectrin, and protein of band 4.1 [67–69].

The erythrocyte membranes used in our experiments were isolated from a fresh human donor blood by the method developed by Dodge et al. [70] and were suspended in a 0.15 M sodium phosphate buffer of pH 7.4. The erythrocyte membranes were depleted of the peripheral proteins of the spectrin–actin network and the proteins of bands 2.1–2.3, 4.1, 4.2, and 6 by the methods described in [71]. The extent of elution of the peripheral proteins was controlled by the method of electrophoresis in a polyacrylamide gel in the presence of sodium dodecyl sulfate (SDS) [72].

Below are the results of investigations of the RTTP of proteins of an erythrocyte membrane in situ in the native state and after depleting them from peripheral proteins – actin–spectrin network (bands 1, 2, and 5) – and the proteins of bands 2.1–2.3, 4.1, 4.2, and 6. We also investigated the capability of the peripheral proteins in solution, extracted from the membranes, to exhibit RTTP.

The RTTP spectrum of a suspension of isolated human erythrocyte membranes has maxima at 415, 441 and 465 nm (Fig. 1, left, curve 1). The decay kinetics of the RTTP of these membranes presented in Fig. 1 (right, curve 1) is clearly multi-exponential and has been adequately approximated by the sum of two exponential components with different lifetimes ( $\tau_1$  and  $\tau_2$ ), amplitudes of lifetime components ( $\alpha_1$  and  $\alpha_2$ ;  $\alpha_1 + \alpha_2 = 1$ ), and contributions of lifetime components to the total emission ( $S_1$  and  $S_2$ ;  $S_1 + S_2 = 1$ ). For the membranes in the native state (control), the RTTP lifetimes are  $\tau_1 = 160$  ms and  $\tau_2 = 1630$  ms,  $\alpha_1 = 0.9$ , and  $S_1 = 0.5$

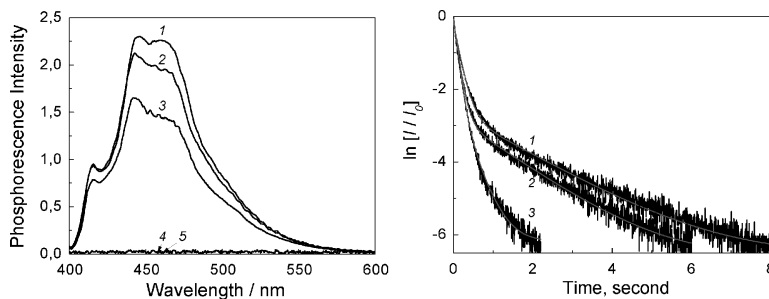


**Fig. 1** Spectra (left) and decay kinetics (right) of RTTP of isolated human erythrocyte membrane suspensions: 1 – intact membranes, 2 – membranes depleted of spectrin and actin, 3 – membranes depleted of bands 2.1–2.3, 4.1, 4.2, 6 (besides spectrin and actin) and extracts of peripheral erythrocyte membrane proteins: 4 – spectrin and actin, 5 – bands 2.1–2.3, 4.1, 4.2, 6. 0.15 M sodium phosphate buffer;  $\lambda_{\text{ex}} = 297$  nm; 20°C

**Table 1** RTTP parameters of suspensions of isolated human erythrocyte membranes with and without peripheral membrane proteins

Isolated human erythrocyte membranes	$\tau_1$ (ms)*	$\tau_2$ (ms)*	$\alpha_1^*$	$S_1^*$
Intact	160	1630	0.91	0.52
Depleted of spectrin and actin	118	1323	0.93	0.55
Depleted of bands 2.1–2.3, 4.1, 4.2, 6 (besides spectrin and actin)	103	330	0.89	0.72

The data are averages of three independent experiments.

\*The standard deviation in these parameters is less than 6%.

(Table 1). The multiexponential character of the kinetic curves defining the decay of the RTTP of the membranes being considered can be explained by the fact that the tryptophanys of the membrane proteins are situated in different environments. These differences, first of all, influence the slow internal dynamics of the proteins. It is likely that internal dynamics of membrane proteins in the vicinity of tryptophanys phosphorescing with the value  $\tau_1$  is more intensive as compared to that at the locations of tryptophan residues phosphorescing with the value  $\tau_2$ . Therefore, the kinetic parameters of the RTTP of isolated erythrocyte membranes reflect the internal dynamics of the protein structure in places of tryptophanyl localization.

To determine the role of protein–protein interactions in the slow internal dynamics of membrane proteins, we investigated the influence of the extraction of peripheral proteins from the erythrocyte membranes on for their RTTP. It has been established that the extraction of the peripheral proteins of the spectrin–actin network from the isolated membranes of human erythrocytes results in a pronounced quenching of the phosphorescence of integral and peripheral proteins remaining in the membrane, which manifests itself by a decrease in the intensity of the RTTP (Fig. 1, left, curve 2) and by an increase in the rate of its quenching (Fig. 1, right, curve 2). Table 1 shows phosphorescence decay parameters of a typical experiment. The data clearly display decrease in lifetime components of the RTTP of erythrocyte membranes, from which spectrin and actin were extracted, as compared to the native membranes; in this case,  $\tau_1$  decreased by approximately 1.4 times and  $\tau_2$  decreased by approximately 1.2 times. The RTTP quenching effect detected evidences that the slow internal dynamics of the membrane proteins is enhanced significantly on the depletion of membranes of spectrin–actin network proteins. Consequently, the proteins of spectrin–actin network significantly limit the slow internal dynamics of membrane proteins in situ. An additional extraction of the remaining peripheral proteins of bands 2.1–2.3, 4.1, 4.2, and 6 from the membranes subjected to the depletion of the spectrin–actin network proteins has caused further decrease in the intensity of the RTTP (Fig. 1, left, curve 3) and its lifetimes (Fig. 1, right, curve 3) to further decrease. The values of  $\tau_1$  and  $\tau_2$  of the RTTP of the depleted membranes were decreased as compared to those of the native membranes:  $\tau_1$  was decreased by approximately 1.6 times and  $\tau_2$  was decreased by approximately 4.9 times (Table 1). This indicates an increased flexibility of the chromophore microenvironment of integral proteins remaining in the membrane. These results provide evidence that



peripheral proteins forming the cytoskeleton not only stabilize the structure of a membrane but also substantially limit the slow internal dynamics of membrane proteins in situ. The extraction of peripheral proteins from the membrane substantially enhances the slow internal dynamics of proteins remaining in it, which is proved by the strong quenching of the RTTP detected in the above-described experiments. It was shown in [73] that the elution of spectrin from an erythrocyte membrane leads to a decrease in the activity of membrane enzymes ( $K^+-Na^+$ -ATPase,  $Ca^{2+}$ -ATPase) and the reassociation of spectrin with the membrane leads to their reactivation. The results of these experiments show that the cytoskeletal proteins of an erythrocyte membrane play an important role in the creation of optimum conditions for the functioning of membrane enzymes. It is conceivable that an important condition for the functioning of membrane proteins in situ is the provision of an optimum level of the amplitude and frequency of fluctuations of the protein structure with the participation of the cytoskeletal proteins.

As the further experiments have shown, the proteins in the composition of native erythrocyte membranes are dramatically distinct from the solutions of the peripheral proteins extracted from the membranes in their capability to exhibit RTTP. Unlike the membrane proteins in situ, the millisecond RTTP of the aqueous extracts of peripheral proteins is strongly quenched and therefore they were not capable of exhibiting long-lived RTTP. As is seen from Fig. 1 (left, curves 4 and 5), the RTTP of aqueous extracts of peripheral proteins was not detectable. These point to the fact that the slow internal dynamics of peripheral membrane proteins in solution is much more intensive than that of the membrane proteins in situ. The data obtained as a result of the investigation of the RTTP of the spectrin-actin network proteins in solution are in good agreement with the data of [13, 35, 36], according to which the RTTP of actin in solution is strongly quenched. The low level of the RTTP of proteins in the composition of a membrane as compared to that of the proteins in solution can be explained by the existence of protein associates in the membrane, the isolation of the proteins included as a compound of the lipid bilayer from the aqueous environment, and the increased content of the rigid  $\alpha$ -helices and  $\beta$ -structures in them.

A suitable experimental approach to the elucidation of the factors controlling the internal dynamics of membrane proteins in situ is the study of the mechanisms of action of detergent on the isolated human erythrocyte membranes by the RTTP method.

Detergents are chaotropic surfactants that can enter membranes, disturb the protein-protein and protein-lipid interactions, and denature the protein by disintegration of its globule. In the case where the content of detergent molecules in a membrane is relatively low, their action results in the appearance of defects in the lipid-matrix packing. As the amount of detergents in a membrane increases, the lipid-packing defects become larger and damage the structural integrity of the membrane, which leads to its subsequent fragmentation. A further increase in the detergent concentration leads to solubilization of the membrane with the formation of lipid-detergent and protein-detergent micelles. In this case, detergent molecules interact with the hydrophobic regions of the membrane proteins and displace the



lipid molecules. The solubilization process manifests itself as a sharp decrease in the light scattering of the membrane suspension. Detergents, depending on their chemical nature, can solubilize membranes with denaturation of proteins or without it. In the case where the concentration of detergents exceeds the critical micelle concentration (CMC), stable micelles consisting of a large number (from several tens to several hundreds) of molecules are formed in the aqueous medium. The CMC of ionic detergents comprises several millimoles and the CMC of the nonionic detergents is smaller by at least one order of magnitude. The action of detergents on membranes is determined by the concentration of their monomeric (not incorporated into the micelles) molecules. Therefore, the ionic detergents having a relatively high CMC, as a rule, more effectively solubilize membranes and more strongly affect the protein conformation than do the nonionic ones [74].

In the present work, we used ionic (anionic) and nonionic detergents having different capabilities to influence the conformation of proteins and disturb the protein–lipid and protein–protein interactions. The ionic detergents used were SDS (Reakhim, Russia), sodium deoxycholate (Serva, Germany), and *N*-lauroylsarcosine Na<sup>+</sup> salt (sarcosyl) (Serva, Germany). The nonionic detergents were digitonin (Merck, USA) and Tween 20 (Serva, Germany). The detergent SDS has a high CMC (1.2–7.1 mM depending on certain conditions) and, therefore, solubilizes membranes to the level of individual lipid and protein macromolecules, disturbs all noncovalent interactions in a protein, and causes a deep denaturation of its globule. The ionic detergent sodium deoxycholate (CMC 1.5 mM) effectively solubilizes the membrane lipids and proteins, including the integral ones; however, it does not denature proteins. The third ionic detergent used in the present work – sarcosyl (CMC 0.54 mM) – damages the structure of proteins in the process of solubilization of a membrane to a minimum extent. Digitonin (CMC 0.087 mM) belongs to nonionic detergents. It is a mildly acting detergent that practically does not change the conformation of membrane proteins. The low CMC (0.06 mM) of the nonionic detergent Tween 20 also exerts its mild (nondenaturing) action on the structure of proteins in the process of solubilization of membranes [74, 75].

In this study, suspensions of membranes were incubated with each of the detergents at varying concentrations during 10 min at 22°C. We controlled the process of solubilization of membranes by detergents using the light-scattering method by measuring the optical density at a wavelength of 530 nm ( $D_{530}$ ).

It was established that an increase in the detergent concentration in a suspension leads, as a rule, to a decrease in the RTTP lifetime of isolated human erythrocyte membranes. Figure 2 (top in left column, curves 1 and 2) shows the ratios of values of  $\tau_1^d$  to  $\tau_1^0$  ( $r_1$ ) and  $\tau_2^d$  to  $\tau_2^0$  ( $r_2$ ) of RTTP, where  $\tau_1^0$  and  $\tau_2^0$  are the phosphorescence lifetimes of isolated human erythrocyte membranes before treatment with detergent (control) and  $\tau_1^d$ ,  $\tau_2^d$  are the phosphorescence lifetimes of isolated human erythrocyte membranes after treatment with detergent. It is seen that when the content of SDS increases to 5 mM, the value of  $r_1$  of the RTTP of the membranes decreases by 1.6 times as compared to the control value. The value of  $r_2$  of the RTTP decreases in the 0–3 mM narrower range of SDS concentrations. When the SDS concentration reaches 3 mM, the value of  $r_2$  of the RTTP of the membranes decreases by

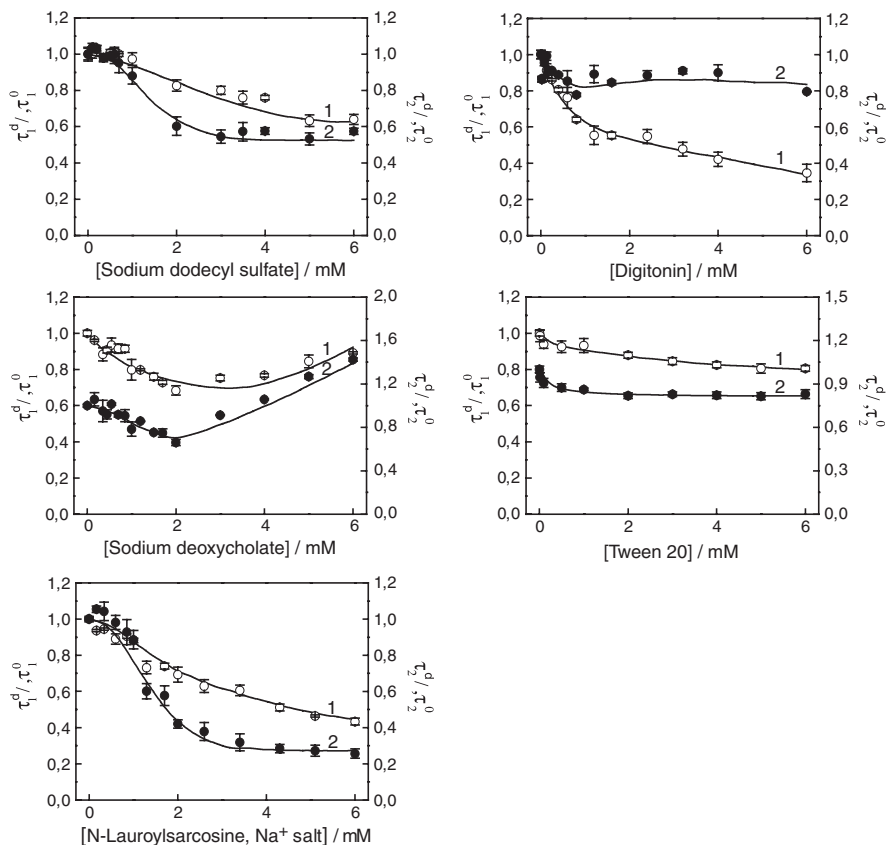


**Fig. 2** The dependence of ratios of  $\tau_1^d/\tau_1^0$  and  $\tau_2^d/\tau_2^0$  on concentration of ionic (left column) and nonionic (right column) detergents in isolated human erythrocyte membrane suspensions.  $\tau_1^0$  and  $\tau_2^0$  are the phosphorescence lifetimes of membranes before treatment with detergent (control) and  $\tau_1^d$  and  $\tau_2^d$  are the phosphorescence lifetimes of membranes after treatment with detergent. Protein concentration is 5 mg/ml; 0.15 M sodium phosphate buffer;  $\lambda_{ex} = 297$  nm; 22°C

1.8 times and retains at this minimum level in the 3–6 mM range of detergent concentrations. Thus phosphorescence lifetimes of isolated human erythrocyte membranes substantially decreases under the action of SDS. The results of investigation of the solubilization activity of SDS by the method of turbidimetry are presented in Fig. 3 (left, curve 1). It is seen that when the SDS concentration reaches 2 mM, a suspension of erythrocyte membranes becomes transparent and the value of  $D_{530}$  approaches zero pointing out that the membranes are totally solubilized.

Sodium deoxycholate influenced differently, depending on its concentration, on kinetics parameters of the RTTP of the erythrocyte membranes (Fig. 2, middle in the left column). When the sodium deoxycholate concentration in a suspension reached 2 mM, the values of  $r_1$  and  $r_2$  of the RTTP decreased approximately by 1.5 times and a further increase in the detergent concentration caused a rise in the lifetimes of

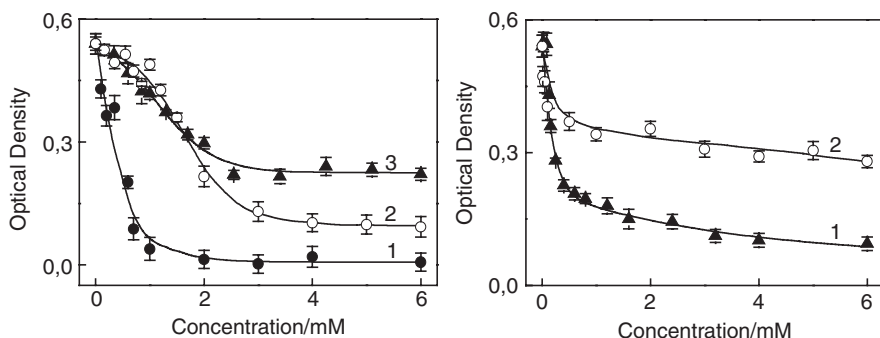


**Fig. 3** The dependence of the optical density at 530 nm on the concentration of ionic (left) and nonionic (right) detergents in isolated human erythrocyte membrane suspensions. Left: 1 – SDS, 2 – sodium deoxycholate, 3 – *N*-lauroylsarcosine Na<sup>+</sup> salt (sarcosyl). Right: 1 – digitonin, 2 – Tween 20. Protein concentration is 0.3 mg/ml; 0.15 M sodium phosphate buffer; 22°C

the RTTP. As is seen from Fig. 3 (left, curve 2), the action of sodium deoxycholate of concentration 0–3 mM on a suspension of erythrocyte membranes leads to its pronounced transparency, decreasing the value of  $D_{530}$  to 0.13. Consequently, sodium deoxycholate is able to solubilize the membranes to the lesser extent in comparison to SDS.

Sarcosyl (0–6 mM) induced a dose-dependent decrease of the value of  $r_1$  of the erythrocyte membranes by approximately 1.6 times (Fig. 2, bottom in the left column, curve 1). In this case, the value of  $r_2$  decreased by approximately 3 times with an increase in the sarcosyl concentration from 0 to 3 mM and remained unchanged when the concentration of the detergent increased further (Fig. 2, bottom in the left column, curve 2). This curve corresponds well to the curve of the dependence of the optical density of a suspension of erythrocyte membranes on the concentration of sarcosyl (Fig. 3, left, curve 3). The degree of transparency of a suspension of erythrocyte membranes treated with sarcosyl was relatively small (as small as  $D_{530} = 0.23$ ) as compared to the degree of transparency of a suspension of erythrocyte membranes treated with SDS and sodium deoxycholate.

The action of digitonin on a suspension of membranes also resulted in quenching of its RTTP (Fig. 2, top in the right column). This effect was most pronounced when the digitonin concentration varied within the range 0–1 mM. When the detergent concentration reached 1 mM, the value of  $r_1$  of the membranes decreased by 1.8 times (Fig. 2, top in the right column, curve 1), and the value of  $r_2$  decreased by 1.12 times (Fig. 2, top in the right column, curve 2). The results of the estimation of the degree of solubilization of the membranes being investigated with the use of digitonin by the decrease in the optical density of their suspension correspond well to the data of phosphorescence investigations. It is seen (Fig. 3, right, curve 1) that the change of transparency of a suspension of erythrocyte membranes (to  $D_{530} = 0.18$ ) is most pronounced in the 0–1 mM range of digitonin concentrations.

As a result of the action of Tween 20 in the concentration range of 0–6 mM on the membranes, the values of  $r_1$  and  $r_2$  were decreased by 1.24 and 1.2 times,

respectively (Fig. 2, bottom in the right column, curves 1 and 2). Phosphorescence lifetimes of membranes decreased most strongly when the Tween 20 content in a suspension increased from 0 to 0.5 mM. In this range of Tween 20 concentrations, the suspension of erythrocyte membranes underwent the major change in transparency (Fig. 3, right, curve 2).

The experimentally detected changes in the values of  $r_1$  and  $r_2$  indicated the quenching of RTTP of erythrocyte membranes under the action of ionic and nonionic detergents (Fig. 2) caused by enhancing of slow internal dynamics of membrane proteins in regions of tryptophan residue localization. The initial portions of the dependences of  $r_1$  and  $r_2$  on the detergent concentration point out the fragmentation of the membranes and their further solubilization. The differences in the behavior of concentration dependences of  $r_1$  and  $r_2$  reflect an individual capability of detergents to solubilize the membrane. The good correspondence between the ranges of detergent concentration, in which the internal dynamics of the membrane proteins was enhanced (the values of  $r_1$  and  $r_2$  were decreased) and the membranes were solubilized (the optical density  $D_{530}$  of the suspension decreased), points to the contingency of processes of the enhancement of the internal dynamics of membrane proteins and the solubilization of membranes.

The following effects can cause an enhancement of the internal dynamics of proteins in the composition of erythrocyte membranes in the process of their solubilization by detergents:

1. Denaturation of the structure of proteins.
2. An increase in the mobility of the molecular surroundings of the proteins due to the dissociation of the protein complexes in the membrane.
3. Transition of proteins from the viscous lipid bilayer of a membrane into the mobile molecular environment.

It is likely that SDS, capable of deeply denaturing proteins and solubilizing membranes to the level of individual molecules of lipids and proteins, enhances the internal dynamics of the membrane proteins through the above-described three mechanisms. According to the light-scattering data, the capability of SDS to clarify a suspension of membranes to a maximum level is due to its better solubilization activity as compared to that of other detergents. Detergents such as sodium deoxycholate, sarcosyl, digitonin, and Tween 20 solubilize membranes without denaturation of the proteins (see above) through the disturbance of the protein-lipid interactions and the destruction of protein associates.

Consequently, the restriction of the internal dynamics of the membrane proteins in situ, as compared to that of the soluble proteins, can be due to the isolation of the macromolecules from the mobile aqueous environment entering into the composition of the viscous lipid bilayer and the existence of protein associates in a membrane. These associates prevent the structure of the proteins from being damaged under the action of a solvent. The assumption that the viscous lipid bilayer of a membrane damps the slow fluctuations of the structure of the membrane proteins is supported by the results of experiments, myelin basic protein did not phosphoresce at room temperature in solution but it showed phosphorescence after being included

into the phosphatidylserine vesicles [10]. In addition to the above-listed factors that limit the internal dynamics of the integral membrane proteins in situ, this dynamics is evidently decreased by the rigid  $\alpha$ -helices and  $\beta$ -strands present in large amounts in the proteins. The transmembrane regions of the integral proteins contain, as a rule, a large amount of ordered structures and are packed more closely than are the soluble proteins [76, 77].

Thus, the low internal dynamics of the membrane proteins in situ, as compared to that of the majority of soluble proteins, can be explained (1) by the presence of protein associates in a membrane, (2) by the isolation of the protein domains from the aqueous environment in the composition of the lipid bilayer, and (3) by the large amount of  $\alpha$ -helices and  $\beta$ -strands in the macromolecules. An increase in the rigidity of the structure of the membrane proteins in situ, caused by the above-described factors, substantially decreases the efficiency of the dynamic quenching of the tryptophan phosphorescence and is responsible for the pronounced capability of the membrane proteins to exhibit a millisecond RTTP.

It has been noted above that the capability of tryptophanlys to exhibit phosphorescence is determined by the phosphorescence quenching amino acid residues located in close proximity to the tryptophanlys (intramolecular quenching). The efficiency of this quenching also depends on the slow internal dynamics of a protein in regions of tryptophan residue localization. Unfortunately, it is not possible to identify the concrete quenchers of phosphorescence of tryptophanlys of membrane proteins because of the absence of necessary X-ray structural analysis data of human erythrocyte membrane proteins. In this respect, soluble proteins with known 3D structures have advantages over the erythrocyte membrane proteins. In the next section, we present results of investigations of the RTTP of lectins, soluble plant proteins.

### 3 Room Temperature Tryptophan Phosphorescence of Plant Lectins in Solution

Lectins are objects of intensive investigations in different fields of biology, medicine, and pharmacology. Representatives of the plant lectin class (concanavalin A, phytohemagglutinin) are widely used in the laboratory practice. These plant proteins are used as pharmaceutical raw materials and are a part of food. Some plant lectins show resistance against high temperatures and proteolytic enzymes and, therefore, can retain their biological activity in food, which is not always healthy [78].

Biological properties of lectins are determined in many respects by their structure. The 3D structure of many lectins is described; however, their slow internal dynamics has not been investigated. As it was noted above, information on the slow internal dynamics of proteins can be obtained from the analysis of its RTTP decay kinetics. In the present section, the results of investigations of plant lectins in solution by the RTTP method are presented. We investigated the following eight lectins: concanavalin A (Con A) from *Canavalia ensiformis* (jack bean),

phytohemagglutinin-L (PHA-L) from *Phaseolus vulgaris* (red kidney bean seeds), wheat germ agglutinin (WGA) from *Triticum* spp. (Wheat germ), peanut agglutinin (PNA) from *Arachis hypogaea* (peanut seed), *Pisum sativum* agglutinin (PSA) from *P. sativum* (pea seed), *Sambucus nigra* agglutinin (SNA-I) from *S. nigra* (elder bark), *Laburnum anagyroides* lectin (LAL) from *L. anagyroides* (bean tree seed), and *Solanum tuberosum* agglutinin (STA) from *S. tuberosum* (potato tuber). All lectins were purchased from Lektinotest (Ukraine) except for Con A, which was from Sigma-Aldrich (USA). Lectins used in our experiments were solvents in 0.15 M sodium phosphate buffer of pH 7.4 and phosphorescence measurements were carried out at 20°C.

The data on the 3D lectin structures have been taken from the Protein Data Bank (PDB) [79] and included the following files: Con A (5CNA), PHA-L (1FAT), WGA (1WGT), PNA (2PEL), and PSA (2LTN). The program RasMol [80] was used to visualize and to analyze the structures. In the present work, we investigated the packing density, i.e., number of atoms ( $N$ ) in the volume of a protein globule at distances of 2–10 Å from the surface of individual tryptophan residues, and the presence of intramolecular quenchers of phosphorescence in their vicinity. We also attempted to identify the tryptophan residues responsible for the room temperature phosphorescence of plant lectins.

### 3.1 Concanavalin A (Con A)

Lectin Con A from the *C. ensiformis* (jack bean) is one of the most known plant lectins. Con A macromolecule consists of four identical subunits, each having a molecular mass of 25.6 kDa. The amino acid sequence of Con A subunit includes four tryptophan residues: Trp-40A, Trp-88A, Trp-109A, and Trp-182A. In Fig. 4a, the structure of the Con A tetramer with the highlighted tryptophan residues, based on the X-ray structural analysis data (file 5CNA in PDB) [81], is presented. According to these data, Trp-88A and Trp-109A are located in the  $\beta$ -strands of the Con A globule and are embedded into it; Trp-40A and Trp-182A are located in the nonstructured regions and are exposed to the solvent.

Con A in solution shows a reliably detectable RTTP. The RTTP spectrum of Con A has maxima at 418, 444, and 461 nm (Fig. 5a). The decay kinetics of the RTTP of Con A is multiexponential and is adequately approximated by the sum of two exponentials with  $\tau_1 = 17$  ms and  $\tau_2 = 520$  ms (Fig. 6a). The values of  $\tau_1$ ,  $\tau_2$ ,  $\alpha_1$ , and  $S_1$  of Con A and other lectins are summarized in Table 2. The biexponential character of the decay kinetics of the RTTP can be explained by the differences in local flexibility of protein structure in regions of tryptophan residue localization and the presence of quenching amino acids in the nearest vicinity of tryptophan residues. Internal dynamics of the protein structure in the vicinity of tryptophan residues is determined by the packing density of the globule, i.e., number of atoms ( $N$ ) in the volume of a protein globule.

The analysis of the X-ray structural data using the RasMol program shows that the packing densities at various distances from the surface of individual

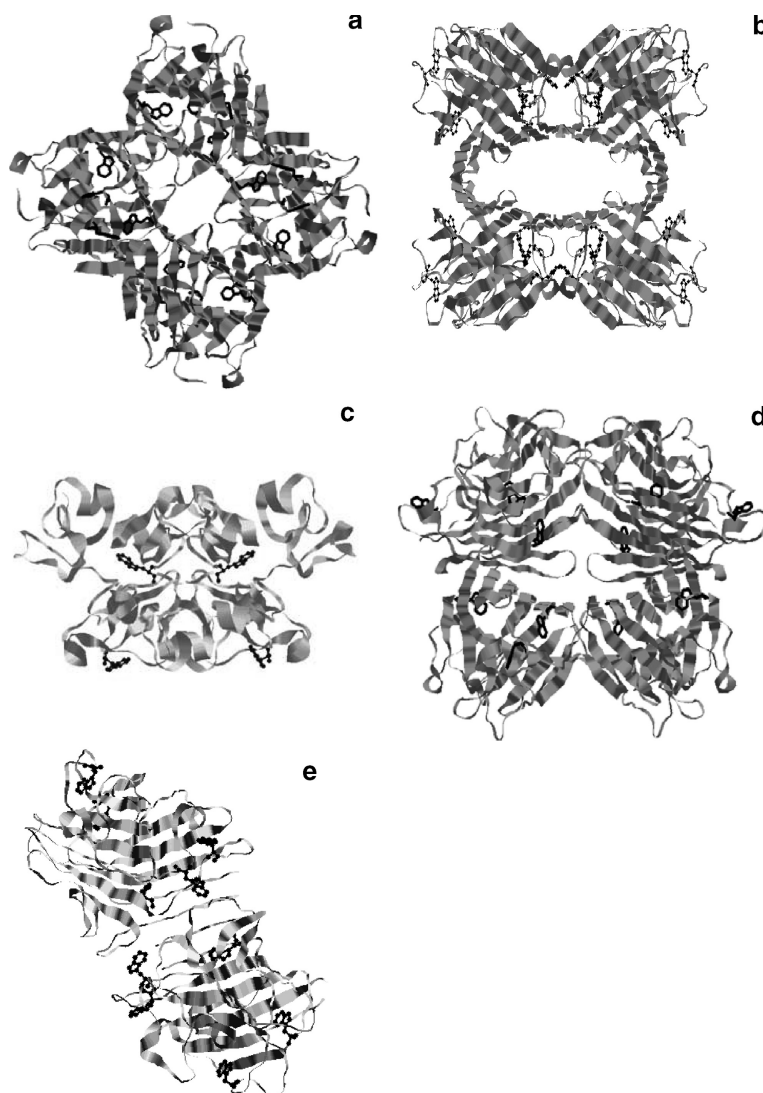
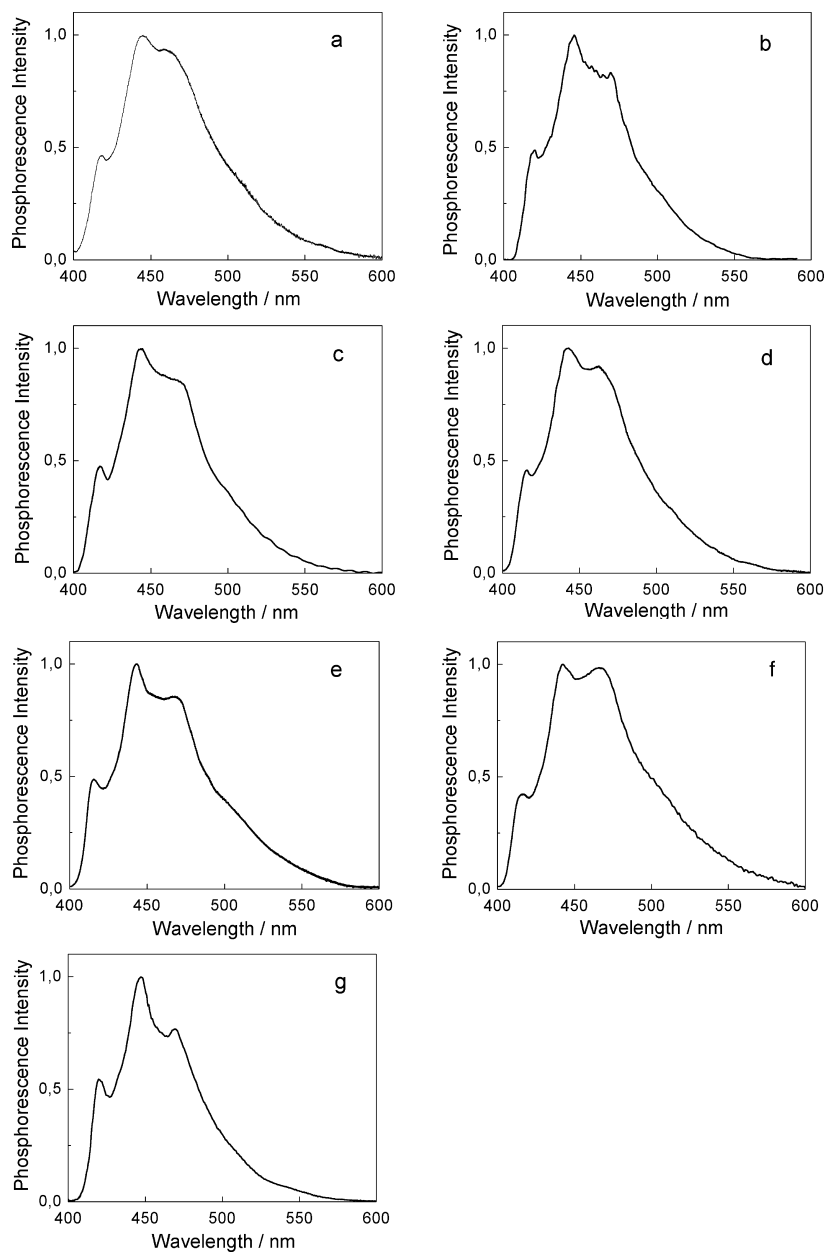


**Fig. 4** Molecular structures of plant lectins: concanavalin A (a), phytohemagglutinin-L (b), wheat germ agglutinin (c), peanut agglutinin (d), and *P. sativum* agglutinin (e)

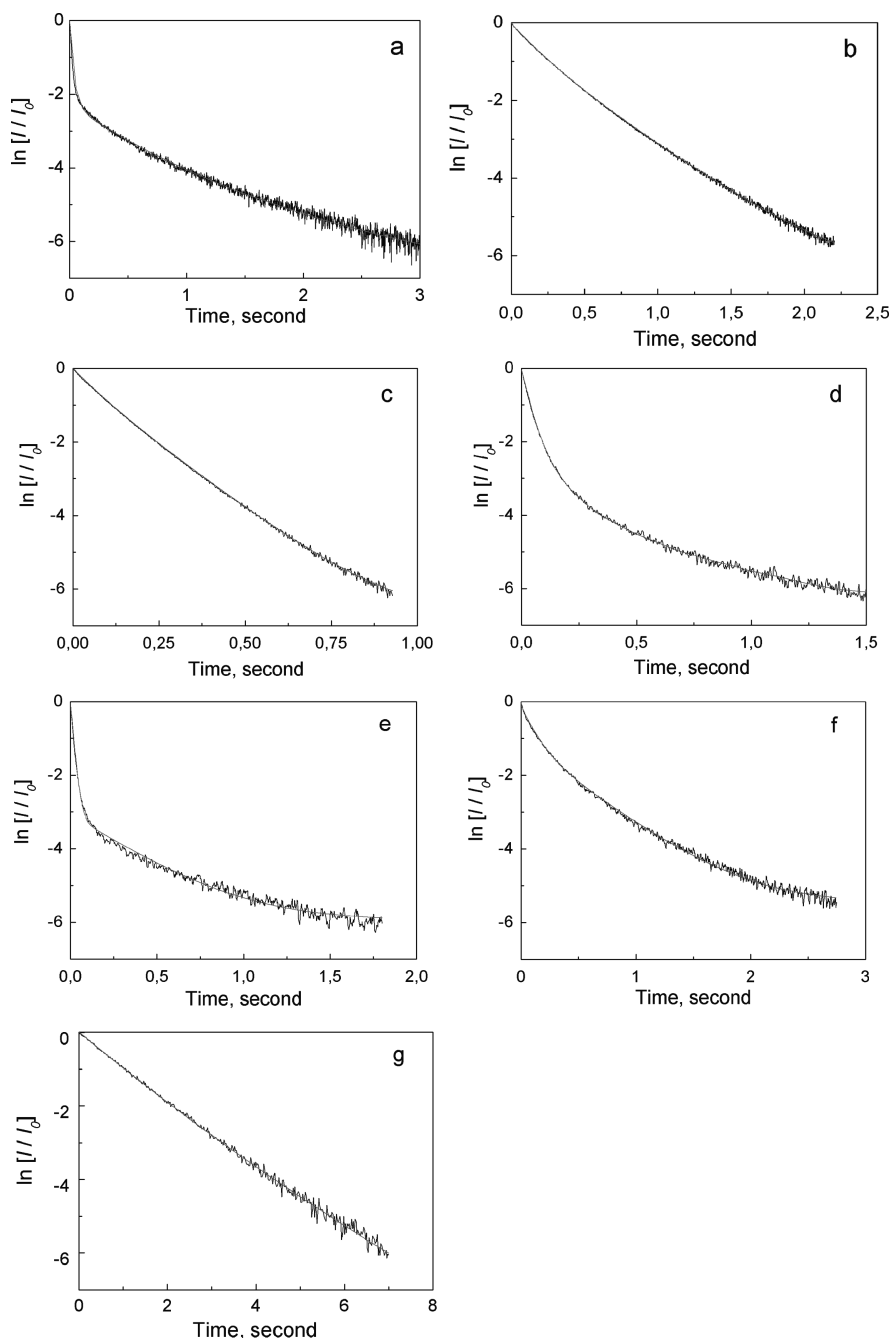
tryptophan residues Trp-40A, Trp-88A, Trp-109A, and Trp-182A are different (Fig.7a). The packing density of Trp-109A microenvironment is the highest. The packing densities of Trp-40A and Trp-88A surroundings are practically equal; however, they are lower than the packing densities of the Trp-109A microenvironment. The lowest packing density was detected in the vicinity of Trp-182A.

Table 3 lists the amino acid residues found at different distances from the surface of individual tryptophan residues of Con A. The table was constructed on the





**Fig. 5** Spectra of RTTP of lectins: concanavalin A (a), leucoagglutinin (b), peanut agglutinin (c), *P. sativum* agglutinin (d), *S. nigra* agglutinin (e), *L. anagyroides* lectin (f), *S. tuberosum* agglutinin (STA) (g)



**Fig. 6** Decay kinetics of RTTP of lectins: concanavalin A (a), leucoagglutinin (b), peanut agglutinin (c), *P. sativum* agglutinin (d), *S. nigra* agglutinin (e), *L. anagyroides* lectin (f), *S. tuberosum* agglutinin (STA) (g)

**Table 2** RTTP lifetimes and maxima of RTTP spectrum of plant lectins

Lectin	Quantity of components	$\tau$ (ms)*	$\tau_1$ (ms)*	$\tau_2$ (ms)*	$\alpha_1$ *	$S_1$ *	$\lambda_1$ (nm)	$\lambda_2$ (nm)	$\lambda_3$ (nm)
Con A	2	–	17	520	0.84	0.25	418	444	461
PHA-L	2	–	190	456	0.52	0.3	420	445	465
WGA	–	–	–	–	–	–	–	–	–
PNA	2	–	73	150	0.38	0.22	418	444	466
PSA	2	–	39	252	0.92	0.64	415	441	463
SNA-I	2	–	18	340	0.95	0.50	416	443	466
LAL	2	–	111	446	0.94	0.30	416	442	467
STA	1	1070	–	–	–	–	417	444	465

The data are averages of three independent experiments.

\*The standard deviation in these parameters is less than 6%.

basis of the X-ray structural analysis data (file 2CNA of PDB) obtained using the RasMol program [81]. As follows from the table, the quenchers of phosphorescence are absent in the region of location of Trp-109A. His-24A, Tyr-22A, and Tyr-64A are found in the microenvironment of Trp-40A. His-180A is located near Trp-182A. These amino acid residues are moderate quenchers (see Sect. 1) of RTTP. The features of the location of the tryptophanys in the Con A globule allow us to conclude that, at room temperature, the Trp-109A residue incorporated into the rigid  $\beta$ -strain shows the long duration phosphorescence corresponding to the lifetime  $\tau_2$ . The packing density in the region of location of this tryptophanyl is the highest as compared to that of the other Con A tryptophanys, and amino acid residues quenching phosphorescence are absent in their microenvironment. Trp-40A and Trp-88A are located in the globule regions with similar atomic packing density. However, the packing density of the surrounding of Trp-40A and Trp-88A is lower as compared to that of Trp-109A. Near Trp-40A, His-24A, Tyr-22A, and Tyr-64A are found, and His-180A is located in the vicinity of Trp-88A. Therefore, it is possible that both residues Trp-40A and Trp-88A can phosphoresce with a lifetime close to  $\tau_1$  at room temperature. It is likely that, at room temperature, Trp-182A does not phosphoresce in the millisecond range. Such a strong quenching of Trp-182A should be due to its location in the highly mobile nonstructured region of the globule, having a low packing density, and the existence of His-180A residues near Trp-182A.

### 3.2 *Phytohemagglutinin-L (PHA-L)*

The structure of lectin PHA-L from *P. vulgaris* (red kidney bean seeds) represents a tetramer consisting of four identical subunits, each having a molecular mass of 27 kDa. The amino acid sequence of PHA-L subunit includes five tryptophanys: Trp-58A, Trp-131A, Trp-153A, Trp-202A, and Trp-226A. Figure 4b presents the structure of the PHA-L tetramer with the indicated tryptophanys, constructed using

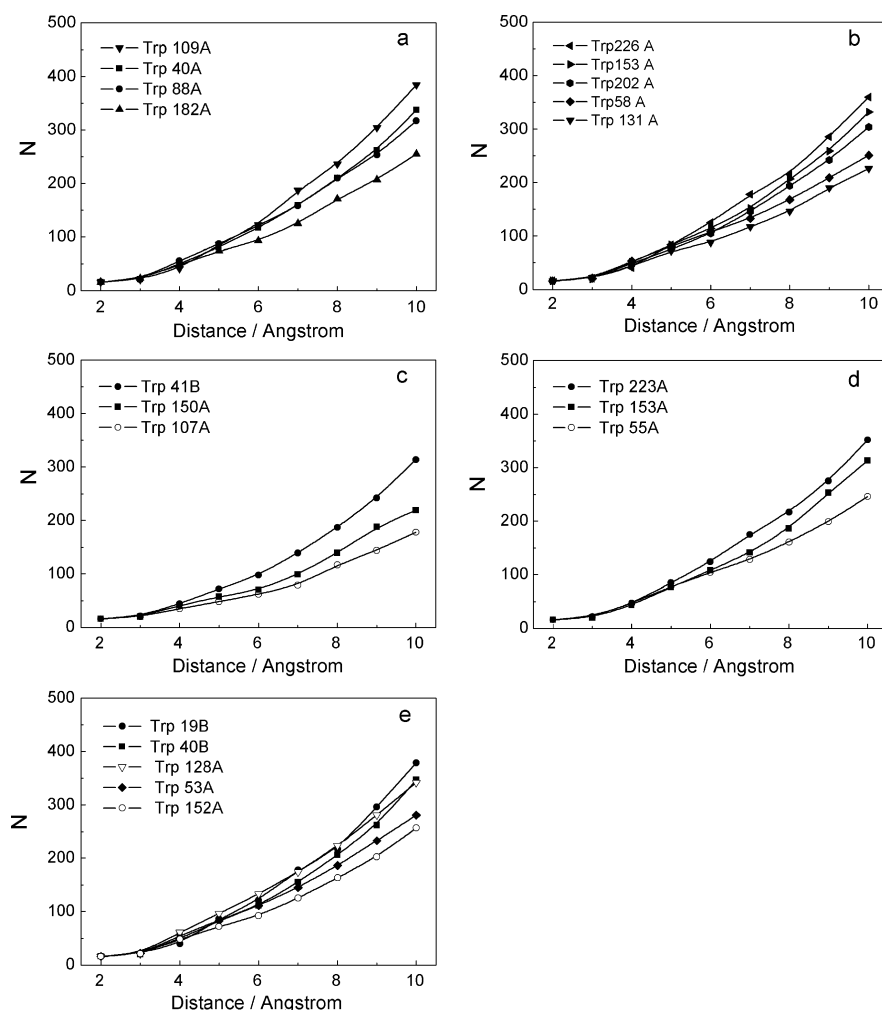


**Fig. 7** The number of atoms ( $N$ ) in the volume of a protein globule at different distances from the surface of individual tryptophan residues of lectins: concanavalin A (a), leucoagglutinin (b), wheat germ agglutinin (c), peanut agglutinin (d), *P. sativum* agglutinin (e)

the RasMol program on the basis of the X-ray structural analysis data (file 1FAT in PDB) [82].

The RTTP spectrum of the PHA-L in solution has maxima at 420, 445, and 465 nm (Fig. 5b). The decay kinetics of the RTTP of PHA-L in solution is multiexponential and is adequately approximated by the sum of two exponentials with  $\tau_1 = 190$  ms and  $\tau_2 = 456$  ms (Fig. 6b). As seen from Fig. 7b, the number of atoms in the surrounding of Trp-58A, Trp-131A, Trp-153A, Trp-202A, and Trp-226A tryptophanys is different. The structure of PHA-L in the regions of

**Table 3** Amino acid residues located at different distances from the concanavalin A tryptophanys. Potential quenchers of phosphorescence are indicated in bold

Å	Trp-40A	Trp-88A	Trp-109A	Trp-182A
2	Asn-41A, Lys-39A	Glu-87, Val-89	Ser-108A, Ser-110A	Glu-183A, Ile-181A
3	Met-42A, Pro-23A		Phe-130A	<b>His-180A</b> , Ley-85A
4	Ala-38A, Asn-41A, <b>His-24A</b> , Ile-25A, Ley-9A, Thr-11A	Asp-136B, Asp-139B, <b>His-180A</b> , Lys-138B, Ile-217A, Pro-86A, Pro-178A, Val-179A	Gly-92A, Leu-93A, Leu-140A, Met-129A, Phe-128A, Phe-175A, Phe-195A, Ser-108A, Val-91A	Asp-82A, Ser-184A
5	Ala-73A, Asp-10A, <b>Tyr-22A</b> , <b>Tyr-64A</b> , Val-65A	Asn-216A, Gln-137B, Ile-181, Ser-134B, Ser-215A	Ala-173A, Ala-193, Leu-154A, Leu-174A, Leu-193A, Phe-111A, Phe-133A, Phe-212A, Thr-194A	Ala-189A, Gly-87A, Leu-81A, Leu-85A, Leu-115A, Pro-86A

location of Trp-58A and Trp-131A is the least densely packed. According to the X-ray structural analysis data, these tryptophanys are located in the nonstructured regions of the PHA-L globule and are exposed to the aqueous surroundings. The protein structure in these regions is usually subject to large thermal fluctuations. Therefore, it may be suggested that Trp-58A and Trp-131A are incapable of exhibiting RTTP with lifetime of more than several milliseconds. The packing density of PHA-L in the regions of location of Trp-153A, Trp-202A, and Trp-226A is much higher, which permits to conclude that these tryptophanys are potentially capable of exhibiting RTTP. In the region where Trp-226A is located, the packing density of the PHA-L globule is the highest. This tryptophanyl is a part of the  $\beta$ -strand and the intramolecular quencher of phosphorescence Tyr-51A is located in its microenvironment. Trp-153A and Trp-202A are located in the nonstructured regions of the PHA-L globule. In the nearest vicinity of Trp-153A, two amino acid residues classified as moderate quenchers of phosphorescence (His-137A and Tyr-180A) are found (Table 4). In the microenvironment of Trp-202A, intramolecular quenchers of phosphorescence are absent. Since it is difficult to take into account all factors influencing the phosphorescence of the PHA-L tryptophanys, the estimation of their actual capability to exhibit RTTP is a challenging task.

**Table 4** Amino acid residues located at different distances from the leucoagglutinin tryptophanys. Potential quenchers of phosphorescence are highlighted in bold

Å	Trp-153A	Trp-202A	Trp-226A
2	Asp-154A, Arg-152A	Glu-201A, Val-203A	Ser-227A, Ser-225A
3	Arg-136A	Thr-14B	Phe-8A, Thr-70A
4	Asp-124A, <b>His-137A</b> , Leu-178A, Phe-123A, Phe-155A, Phe-187A, Thr-125A, Thr-151A, <b>Tyr-180A</b>	Asn-12B, Asn-15B, Gln-56A, Glu-201A, Ile-55A, Pro-54A, Pro-94A, Pro-200A, Ser-204A, Val-95A, Val-203A	Asn-7A, Glu-206A, Phe-6A, Phe-11A, Phe-207A, Ser-71A, Val-205A
5	Ile-138A, Phe-74A	Ile-57A, Thr-202A, Val-93A	Ley-16A, Ley-224A, Phe-72A, Phe-90A, Phe-228A, <b>Tyr-51A</b> , Val-223A

### 3.3 Wheat Germ Agglutinin (WGA)

Lectin WGA from the *Triticum* spp. (wheat germ) consists of two identical subunits, each having a molecular mass of 18.6 kDa. The amino acid sequence of these subunits includes three tryptophanys generally capable of exhibiting RTTP: Trp-41B, Trp-107A, and Trp-150A. However, we failed to detect the RTTP of WGA in the millisecond range. The actual reasons for the strong quenching of the RTTP can be the high mobility of the WGA tryptophanyl micro surrounding and the existence of

static quenchers in the nearest vicinity of them. The structure of the WGA dimer, constructed using the RasMol program based on the X-ray structural analysis data (file 1WGT in PDB) [83], is presented in Fig. 4c.

According to the X-ray structural analysis data, Trp-41B, Trp-107A, and Trp-150A are located in the nonstructured region at the periphery of the WGA globule. The packing density of the protein globule in the regions where the three WGA tryptophanys are located is shown in Fig. 7c. It follows from the figure that the packing density of the surrounding of Trp-107A and Trp-150A of WGA is not high. Approximately the same packing density is characteristic of Trp-182A of Con A as well as Trp-58A and Trp-131A of PHA-L, all of which, as it was shown above, are incapable of exhibiting the millisecond phosphorescence at room temperature. Since quenchers of phosphorescence are absent in the regions of location of Trp-107A and Trp-150A of WGA (Table 5), the most probable reason for the pronounced quenching of their phosphorescence is the strong fluctuation of the protein structure with a millisecond characteristic time. Even though the packing density of atoms at the location of Trp-41B is higher than that at the location of Trp-107A and Trp-150A, the strong quenchers of phosphorescence Cys-31B, Cys-40B, and Cys-126A, located in the nearest vicinity of Trp-41B, apparently disable this WGA tryptophanyl to exhibit RTTP.

**Table 5** Amino acid residues located at different distances from the wheat germ agglutinin tryptophanys. Potential quenchers of phosphorescence are highlighted in bold

Å	Trp-41B	Trp-107A	Trp-150A
2	Thr-42B, <b>Cys-40B</b>	Gln-106A, Gly-108A	Gly-151A
3			Lys-149A
4	Ala-39A, Ala-125B, <b>Cys-31B, Cys-126A,</b> Glu-27A, Glu-28B, Gly-28B, Gly-32B, Ser-43B, Ser-127B	Gln-92A, Tyr-109A	Asp-29B, Gly-158A, Ser-148A, Ser-152A, <b>Tyr-159A</b>
5	Asp-12BA	Gln-122A	Asp-135A, Gln-165A

### 3.4 Peanut Agglutinin (PNA)

Lectin PNA from *A. hypogaea* (peanut seed) represents a tetramer consisting of four identical subunits, each having a molecular mass of 25 kDa. The amino acid sequence of a PNA subunit includes three tryptophanys: Trp-55A, Trp-153A, and Trp-223A. In Fig. 4d, the structure of the PNA tetramer with the highlighted tryptophanys, constructed using the RasMol program based on X-ray structural analysis data (file 2PEL in PDB) [84], is presented. According to the X-ray structural analysis data, Trp-223A is incorporated into the  $\beta$ -strand and is embedded into the interior of the PNA globule. Trp-153A is also incorporated into the  $\beta$ -strand. The Trp-55A is located in the nonstructured region of the PNA globule, closer to its periphery.



It has been established that PNA in solution exhibits a reliably detectable RTTP. The RTTP spectrum of PNA in solution has maxima at 418, 444, and 466 nm (Fig. 5c). The decay kinetics of the RTTP of PNA in solution is multiexponential and is adequately approximated by the sum of two exponentials (Fig. 6c) and is characterized by the following lifetimes:  $\tau_1 = 73$  ms,  $\tau_2 = 150$  ms (Table 2). As is seen from Fig. 7d, the packing densities of the PNA globule at the localization of the PNA Trp-55A, Trp-153A, and Trp-223A are different. The packing density is relatively high for Trp-223A and Trp-153A and is low for Trp-55A.

Table 6 presents the amino acid residues found at different distances from the surface of the PNA tryptophanlys. As follows from the table, static quenchers of phosphorescence are absent in the microenvironment of Trp-55A. His-137A is located in the nearest vicinity of Trp-153A, while Tyr-48A is located near Trp-223A. Despite the presence of the static quencher near Trp-223A, this tryptophanyl residue may phosphoresce at room temperature with a lifetime close to  $\tau_2$  because it is located in the most densely packed region of the PNA globule and incorporated into the  $\beta$ -strand. The packing density in the vicinity of Trp-153A is lower than that of Trp-223A (Fig. 7d). This gives reasons to expect that Trp-153A, also incorporated into the  $\beta$ -strand, is capable of exhibiting phosphorescence at room temperature with a lifetime close to  $\tau_1$ . It seems likely that Trp-55A located in the nonstructured region at the periphery of the PNA globule with a sparse packing of atoms does not phosphoresce at room temperature in the millisecond range.

**Table 6** Amino acid residues located at different distances from the peanut agglutinin tryptophanlys. Potential quenchers of phosphorescence are highlighted in bold type

Å	Trp-55A	Trp-153A	Trp-223A
2	Ile-54A, Ser-56A	Asn-154A, Pro-152A	Ser-222A, Ser-224A
3	Leu-198A		Phe-8A, Thr-67A
4	Asn-61A, Arg-53A, Glu-200A, Leu-198A, Lys-195A, Pro-199A, Ser-57A	Asp-136A, Asn-180A, <b>His-137A</b> , Ser-155A, Thr-185A, Thr-186A, Phe-122A, Val-138A, Val-151A, Val-178A	Asn-7A, Phe-6A, Phe-69A, Phe-204A, Phe-206A, <b>Tyr-48A</b>
5	Ala-63A, Leu-194A, Leu-229A, Val-62A	Asp-123A, Met-173A, Thr-124A, Thr-135A, Val-161A	Arg-221A, Gly-205A, Ile-220A, Leu-47A, Phe-11A, Phe-87A, Phe-225A, Ser-68A

### 3.5 *Pisum sativum* Agglutinin (PSA)

Lectin PSA lectin from *P. sativum* (pea seed) consists of two identical subunits, each having a molecular mass of 25.2 kDa. The amino acid sequence of a PSA subunit

includes five tryptophanys: Trp-19B, Trp-40B, Trp-53A, Trp-128A, and Trp-152A. In Fig. 4e, the structure of the PSA dimer with the highlighted tryptophanys, constructed using the RasMol program based on the X-ray structural analysis data (file 2LTN in PDB) [85], is presented. Table 7 presents the amino acid residues found in the vicinity of the PSA tryptophanys.

PSA in solution is capable of exhibiting millisecond RTTP. The RTTP spectrum of PSA has maxima at 415, 441 and 463 nm (Fig. 5d). The decay kinetics of RTTP of PSA is multiexponential. It is adequately approximated by the sum of two exponentials (Fig. 6d) with  $\tau_1 = 39$  ms and  $\tau_2 = 252$  ms (Table 2). Tryptophanys of PSA are different in packing density in the regions of its location. Unfortunately, identification of PSA tryptophanys capable of exhibiting phosphorescence at room temperature is very difficult because of the presence of amino acid residues quenching phosphorescence in their microenvironment. Out of the five tryptophanys, only Trp-53A is included in the  $\beta$ -strand. However, distal position of Trp-53A and relatively low packing density in the region of its location (Fig. 7e) did not allow establishing its capability to exhibit phosphorescence at room temperature.

**Table 7** Amino acid residues located at different distances from the *P. sativum* agglutinin tryptophanys. Potential quenchers of phosphorescence are highlighted in bold

Å	Trp-19B	Trp-40B	Trp-53A	Trp-128A	Trp-152A
2	Gly-18B	Ser-39B, Ser-41B	Asp-54A, Ile-52A	Ala-127A, Asp-129A	Lys-153A, Ser-151A
3	Val-20B,	Ile-8A, Thr-65A	Glu-18B, Val-16B		Arg-135A
4	Asn-17C, <b>His-51A</b> , Gln-15C, Gln-16C, Ile-50A, Pro-17B, Pro-49A,	Ile-22B, Leu-7A, Phe-6A, Phe-24B, Ser-66A	Arg-55A, Asn-59A, <b>His-51A</b> , Lys-13B, Pro-17B, Val-60A	Asn-125A, Glu-99A, Ile-144A, Lys-145A, <b>Tyr-100A</b>	Asp-121A, <b>His-136A</b> , Ile-71A, Ile-137A, Leu-154A, Leu-177A, Lys-150A, Phe-120A, Thr-122A, <b>Tyr-4B</b> , <b>Tyr-174A</b>
5	Ala-88A, Asp-14C, Asn-17C, Glu 2A, Pro-89A, Ser-12C, Val-90A	Gly-23B, Leu-18A, Phe-11A, Phe-42B, Phe-67A, Phe-85A, <b>Tyr-46A</b> , Val-37B	Ala-61A, Leu-12B, Leu-46B	Ala-107A	Phe-69A

### 3.6 *Sambucus nigra* Agglutinin (SNA-I)

Lectin SNA-I lectin from *S. nigra* (elder bark) is a tetramer. The molecular mass of the SNA-I tetramer is equal to 140 kDa. The subunits of this lectin are connected by disulfide bonds. Figure 5e shows the RTTP spectrum of SNA-I lectin in aqueous solution. As in the case of the above-described lectins, the RTTP spectrum of SNA-I has the maxima at 416, 443, and 466 nm. The decay kinetics of the RTTP of SNA-I in solution is multiexponential and adequately approximated by the sum of two exponentials (Fig. 6e) with  $\tau_1 = 18$  ms and  $\tau_2 = 340$  ms (Table 2). Unfortunately, the 3D structure of SNA-I is not available to date and therefore, we could not analyze the amino acid sequence, the packing density near the tryptophan residues, the presence of quenchers, and the tryptophanyls responsible for the RTTP of this lectin.

### 3.7 *Laburnum anagyroides* Lectin (LAL)

It was established that lectin LAL from *L. anagyroides* (bean tree seed) in solution is capable of exhibiting RTTP. As is seen, its RTTP spectrum has maxima at 416, 442, and 467 nm (Fig. 5f). The decay kinetics of the RTTP of LAL lectin is multiexponential (Fig. 6f) and adequately approximated by the sum of two exponentials with  $\tau_1 = 111$  ms and  $\tau_2 = 446$  ms (Table 2), which points to the fact that the properties of the surroundings of the tryptophanyls capable of exhibiting RTTP are heterogeneous. These differences, first of all, can be due to differences in packing density between the regions of location of the tryptophanyls in the LAL globule and the presence of the amino acid residues, representing potential quenchers of phosphorescence, in their nearest environment. However, as for SNA-I, at present, the 3D structure of LAL has not been yet determined, hence the analysis of the features of the localization of the tryptophanyls in the LAL globule and the identification of the tryptophan residues phosphorescing at room temperature with different lifetimes are impossible.

### 3.8 *Solanum tuberosum* Agglutinin (STA)

Figure 5g represents the RTTP spectrum of lectin STA extracted from *S. tuberosum* (potato tuber) in solution. Figure 6g presents the monoexponential decay kinetics of the RTTP of STA in solution with  $\tau = 1070$  ms. The large (for the protein in solution) lifetime of the RTTP of STA (more than 1 s) points to an extremely high packing density of atoms at the location of the tryptophanyl responsible for the phosphorescence and, consequently, to a high rigidity of the structure of the hydrophobic core of the STA globule in the region of location of this tryptophanyl. Unfortunately, the absence of X-ray structural analysis data on the STA structure gives no way to discuss the features of the location of the tryptophanyls in the STA globule and their capability to exhibit RTTP in detail.

Thus, as a result of the above-described works, the RTTP of seven of the eight plant lectins have been detected for the first time. They are as follows: Con A from *C. ensiformis* (jack bean), PHA-L from *P. vulgaris* (red kidney bean seeds), PNA from *A. hypogaea* (peanut seed), PSA from *P. sativum* (pea seed), SNA-I from *S. nigra* (elder bark), LAL from *L. anagyroides* (bean tree seed), and STA from *S. tuberosum* (potato tuber).

It has been established that RTTP decay kinetics of lectins, depending on the characteristic features of their tryptophan residues localization, can be adequately approximated by the sum of two exponentials (Con A, PHA-L, PNA, PSA, SNA-I, LAL) or one exponential (STA).

On the basis of 3D protein structures taken from the PDB, the features of the location of the tryptophan residues of plant lectins have been analyzed and their capability for the phosphorescence at room temperature has been discussed taking into account the packing density of atoms in the lectin globule and the existence amino-acid residues possessing the properties of static quenchers of phosphorescence. The relatively large values of the lifetimes of the RTTP of the plant lectins in solution point to the notion that the slow internal dynamics of these lectins is smaller than that of the majority of proteins in solution which are incapable of exhibiting long-lived RTTP. It can be explained by the high content of  $\beta$ -strands in the plant lectins. The high conformational rigidity of these lectins is probably a reason for their resistance to the action of temperature and to other physico-chemical factors.

In conclusion, it is necessary to note that the "RTTP" abbreviation is not always used in the literature. In works devoted to the tryptophan phosphorescence at room temperature, the abbreviation "RTP" (room temperature phosphorescence) is frequently used. In our opinion it is preferable to use the abbreviation "RTTP" for the following reasons:

1. Except for tryptophanlys, tyrosine residues of proteins may also phosphoresce at room temperature [86].
2. In biological membranes and cells, apart from proteins, the lipid peroxidation (LPO) products are capable of exhibiting room temperature phosphorescence. Excitation spectra of room temperature phosphorescence of LPO products are localized in the spectral range of 240–420 nm. LPO products phosphoresce at room temperature in the range of 420–600 nm [6, 87–91].

Taking into account that in biological objects not only tryptophanlys but also other chromophores are capable of exhibiting room temperature phosphorescence, the use of the abbreviation "RTTP" better defines the nature of the phosphorescence.

**Acknowledgment** This work is supported by International Science and Technology Center, Grant B-1332.

## References

1. S. V. Konev, *Fluorescence and phosphorescence of proteins and nucleic acids* (Plenum Press, New York, 1967).
2. A. P. Demchenko, Fluorescence and dynamics in proteins, in *Topics in fluorescence spectroscopy*, **Vol. 3**, edited by J. R. Lakowicz (Plenum Press, New York, 1992) pp. 65–111.
3. J. R. Lakowicz, *Principles of fluorescence spectroscopy*, 2nd edn. (Kluwer Academic/Plenum Publishers, New York, 2000).
4. S. V. Konev, V. P. Bobrovich, About the phosphorescence spectrums of proteins at different temperatures, *Dokl. Acad. Nauk BSSR* **10**, 786–788 (1966).
5. M. L. Saviotti, W. C. Galley, Room temperature phosphorescence and the dynamic aspects of protein structure, *Proc. Natl. Acad. Sci. U S A* **71**(10), 4154–4158 (1974).
6. V. M. Mazhul', Yu. S. Ermolaev, V. A. Bobrov, V. P. Nicolskaya, S. V. Konev, About the conformational sensibility of the parameters of tryptophan phosphorescence at room temperature of proteins of membranes and cells, *Vesti Acad. Navuk BSSR, Ser. Biyal. Navuk* **6**, 52–56 (1976).
7. Y. Kai, K. Imacubo, Temperature dependence of the phosphorescence lifetimes of heterogeneous tryptophan residues in globular proteins between 293 and 77 K, *Photochem. Photobiol.* **29**, 261–265 (1979).
8. V. M. Mazhul', Yu. S. Ermolaev, S. V. Konev, Tryptophan phosphorescence at room temperature. A new method for studying the structural state of biological membranes and proteins in cell, *J. Appl. Spectrosc.* **32** (5), 530–534 (1980).
9. V. M. Mazhul', Yu. S. Ermolaev, S. V. Konev, M. A. Martynova, V. P. Nicolskaya, Zh. V. Prokopova, Investigated of internal dynamics of proteins by the method of tryptophan phosphorescence at room temperature, *Biofizika* **28** (6), 980–988 (1983).
10. J. Vanderkooi, J. W. Berger, Excited triplet states used to study biological macromolecules at room temperature, *Biochim. Biophys. Acta* **976**, 1–27 (1989).
11. G. B. Strambini, Tryptophan phosphorescence as a monitor of protein flexibility, *J. Mol. Liq.* **42**, 155–165 (1989).
12. G. B. Strambini, E. Gabellieri, Temperature dependence tryptophan phosphorescence in proteins, *Photochem. Photobiol.* **51**, 643–648 (1990).
13. G. B. Strambini, S. S. Lehrer, Tryptophan phosphorescence of G-actin and F-actin, *Eur. J. Biochem.* **159**, 645–651 (1991).
14. J. M. Vanderkooi, Tryptophan phosphorescence from proteins at room temperature, in *Topics in fluorescence spectroscopy*, **Vol. 3**, edited by J. R. Lakowicz (Plenum Press, New York, 1992) pp. 113–136.
15. G. B. Strambini, M. Gonnelli, Tryptophan phosphorescence in fluid solution, *J. Am. Chem. Soc.* **117**, 7646–7651 (1995).
16. M. Gonnelli, G. B. Strambini, Phosphorescence lifetime of tryptophan in proteins, *Biochemistry* **34**, 13847–13857 (1995).
17. V. Subramaniam, A. Gafni, D. G. Steel, Time-resolved tryptophan phosphorescence spectroscopy: A sensitive probe of protein folding and structure, *IEEE J. Sel. Top. Quant. Electron.* **2**(4), 1107–1114 (1996).
18. Z. Li, A. Bruce, W. C. Galley, Temperature dependence of the disulfide perturbation to the triplet state of tryptophan, *Biophys. J.* **61**, 1364–1371 (1992).
19. F. Tolgyesi, B. Ullrich, J. Fidy, Tryptophan phosphorescence signals characteristic changes in protein dynamics at physiological temperature, *Biochim. Biophys. Acta* **1435**, 1–6 (1999).
20. A. Gershenson, J. A. Shauerte, L. Giver, F. H. Arnold, Tryptophan phosphorescence study of enzyme flexibility and unfolding in laboratory-evolved thermostable esterases, *Biochemistry* **39**, 4658–4665 (2000).

21. V. M. Mazhul', E. M. Zaitseva, D. G. Shcherbin, Intramolecular dynamics and functional activity of proteins, *Biophysics* **45**(6), 935–959 (2000).
22. A. A. Sukhodola, G. B. Tolstorozhev, V. A. Shashilov, V. M. Mazhul', D. G. Shcherbin, E. M. Zaitseva, Room-temperature phosphorescence of indole, tryptophan and their derivatives in solid films, in *Abstracts of 9<sup>th</sup> European conference on the spectroscopy of biological molecules* (Prague, 2001) p. 224.
23. V. M. Mazhul', E. M. Zaitseva, D. G. Shcherbin, Phosphorescence of tryptophan residues of proteins at room temperature, *J. Appl. Spectrosc.* **69**(2), 213–219 (2002).
24. M. Gonnelli, G. B. Strambini, Structure and dynamics of proteins encapsulated in silica hydrogels by Trp phosphorescence, *Biophys. Chem.* **104**, 155–169 (2003).
25. G. B. Strambini, M. Gonnelli, Effects of urea and guanidine hydrochloride on the activity and dynamical structure of equine liver alcohol dehydrogenase, *Biochemistry* **25**, 2471–2476 (1986).
26. V. M. Mazhul', I. V. Mjakinnik, A. N. Volkova, Intramolecular dynamics of structure of alkaline phosphatase from *Escherichia coli*, *Proc. SPIE* **2370**, 706–710 (1994).
27. V. Subramaniam, N. C. H. Bergenhem, A. Gafni, D. G. Steel, Phosphorescence reveals a continued slow annealing of the protein core following reactivation of *Escherichia coli* alkaline phosphatase, *Biochemistry* **34**, 1133–1136 (1995).
28. V. Subramaniam, D. G. Steel, A. Gafni, In vitro renaturation of beta-lactoglobulin A leads to a biologically active but incompletely refolded state, *Protein Sci.* **5**, 2089–2094 (1996).
29. S. Zh. Kananovich, V. M. Mazhul', Effect of urea and high temperatures on conformation, internal dynamics and enzyme activity of *Escherichia coli* alkaline phosphatase, in *Book of abstracts the Minerva-Gentner symposium on optical spectroscopy of biomolecular dynamics* (Kloster Banz, Bad Staffelstein, 2004) p. 106.
30. S. G. Kananovich, V. M. Mazhul', Structure and enzyme activity of *Escherichia coli* alkaline phosphatase at the action of urea, in *Abstracts of 9<sup>th</sup> International Summer School on Biophysics "Supramolecular structure and function"* (Rovinj, 2006) p. 136.
31. S. G. Kananovich, V. M. Mazhul', Unfolding and refolding of *Escherichia coli* alkaline phosphatase, in *The 5<sup>th</sup> International conference on biological physics* (Gothenburg, 2004), B 05-193, p. 39.
32. J. V. Mersol, D. G. Steel, A. Gafni, Detection of intermediate protein conformations by room temperature tryptophan phosphorescence spectroscopy during denaturation of *Escherichia coli* alkaline phosphatase, *Biophys. Chem.* **48**, 281–291 (1993).
33. V. M. Mazhul', S. Zh. Kananovich, On the ability of a protein to exist in many partially folded states, *Biophysics* **49**(3), 392–402 (2004).
34. V. M. Mazhul', S. Zh. Kananovich, Effect of temperature on the internal dynamics and the conformational state of bacterial alkaline phosphatase, *Biophysics* **51**(3) 364–369 (2006).
35. V. M. Mazhul', E. M. Zaitseva, M. M. Shavlovsky, I. M. Kuznetsova, K. K. Turoverov, Tryptophan phosphorescence of native and inactivated actin, *Biophysics* **46**(6), 988–996 (2001).
36. V. M. Mazhul', E. M. Zaitseva, M. M. Shavlovsky, O. V. Stepanenko, I. M. Kuznetsova, K. K. Turoverov, Monitoring of actin unfolding by room temperature tryptophan phosphorescence, *Biochemistry* **42**, 13551–13557 (2003).
37. M. Gonnelli, G. B. Strambini, Glycerol effects on protein flexibility: A tryptophan phosphorescence study, *Biophys. J.* **65**, 131–137 (1993).
38. W. W. Wright, G. N. Guffanti, J. M. Vanderkooi, Protein in sugar films and in glycerol/water as examined by infrared spectroscopy and by the fluorescence and phosphorescence of tryptophan, *Biophys. J.* **85**, 1980–1995 (2003).
39. P. Cioni, G. B. Strambini, Pressure effect on protein flexibility monomeric proteins, *J. Mol. Biol.* **242**, 291–301 (1994).
40. V. M. Mazhul', E. M. Zaitseva, The new mechanism of enzyme activity regulation by ionic strength, *J. Biosci.* **24**(1), 53 (1999).

41. V. M. Mazhul', E. M. Zaitseva, D. G. Shcherbin, Effects of ionic strength and temperature on large-scale internal dynamics of liver alcohol dehydrogenase, in *Abstracts of 7<sup>th</sup> conference on methods and applications of fluorescence* (Amsterdam, 2001) p. 134.
42. E. M. Zaitseva, V. M. Mazhul', pH-induced changes in aldolase internal dynamics and conformation: Fluorescence and phosphorescence study, in *Abstracts of 7<sup>th</sup> conference on methods and applications of fluorescence* (Amsterdam, 2001) p. 210.
43. E. M. Zaitseva, V. M. Mazhul', Internal dynamics of aldolase probed by room temperature time-resolved tryptophan phosphorescence, in *Abstracts of 4<sup>th</sup> international conference on biological physics* (Kyoto, 2001) p. 104.
44. G. B. Strambini, M. Gonnelli, Tryptophan luminescence from liver alcohol dehydrogenase in its complexes with coenzyme. A comparative study of protein conformation in solution, *Biochemistry* **29**, 196–203 (1990).
45. A. Baracca, E. Gabillieri, S. Barogi, G. Solani, Conformational changes of the mitochondrial F<sub>1</sub>-ATPase  $\epsilon$ -subunit induced by nucleotide binding as observed by phosphorescence spectroscopy, *J. Biol. Chem.* **270**(37), 21845–21851 (1995).
46. V. M. Mazhul', E. M. Zaitseva, L. G. Mitskevich, N. V. Fedurkina, B. I. Kurganov, Effects of ligands binding on muscle glycogen phosphorylase *b* internal dynamics, *J. Biosci.* **24**(1), 53 (1999).
47. V. M. Mazhul', E. M. Zaitseva, L. G. Mitskevich, N. V. Fedurkina, B. I. Kurganov, Phosphorescence analysis of the intramolecular dynamics of muscle glycogen phosphorylase *b*, *Biophysics* **44**(6), 975–981 (1999).
48. B. I. Kurganov, N. V. Fedurkina, L. G. Mitskevich, V. M. Mazhul', E. M. Zaitseva, Study of muscle glycogen phosphorylase *b* association by means of tryptophan phosphorescence at room temperature, *Dokl. Biophys.* **367–369**, 67–70 (1999).
49. S. Zh. Kananovich, V. M. Mazhul'. Fluorimetric analysis of the structural-dynamic state of alkaline phosphatase of *Escherichia coli*, *J. Appl. Spectrosc.* **70**(5), 673–677 (2003).
50. P. Cioni, L. Piras, G. B. Strambini, Tryptophan phosphorescence as a monitor of the structural role of metal ions in alkaline phosphatase, *Eur. J. Biochem.* **185**, 573–579 (1989).
51. S. Zh. Kananovich, V. M. Mazhul', Effect of proteolysis on the internal dynamics of *Escherichia coli* alkaline phosphatase tested by the room-temperature phosphorescence method, in *Abstracts of 9<sup>th</sup> European conference on the spectroscopy of biological molecules* (Prague, 2001) p. 61.
52. T. Horie, J. M. Vanderkooi, Phosphorescence of alkaline phosphatase of *E. coli* in vitro and in situ, *Biochim. Biophys. Acta* **670**, 294–297 (1981).
53. V. M. Mazhul', S. Zh. Kananovich, Zh. V. Prokopova, Internal dynamics of membrane and cytoplasmic proteins of germ of *Escherichia coli*, *Vesti Acad. Navuk BSSR, Ser. Biyal. Navuk* **1**, 60–64 (2001).
54. V. M. Mazhul', D. G. Shcherbin, Tryptophan phosphorescence as monitor of flexibility of membrane proteins in cells, *Proc. SPIE* **2980**, 487–494 (1987).
55. V. M. Mazhul', V. N. Kalunov, V. A. Buravskii, A. N. Volkova, R. I. Gronskeya, Phosphorescent analysis of the growth factors action to the internal dynamics of membrane proteins of rat pheochromocytomas PC12 cells, *Dokl. Acad. Nauk BSSR* **39**(6) 83–86 (1995).
56. V. M. Mazhul', Zh. V. Prokopova, L. S. Ivashkevich. Mechanisms of the action of the humic preparations and peat on the functional activity of the cells, in *Humic substances in biosphere* (Nauka, Moscow, 1993) pp. 16–23.
57. V. Mazhul', D. Shcherbin, I. Zavodnik, K. Rękawecka, M. Bryszewska, The effect of oxidative stress induced by *t*-butyl hydroperoxide on structural dynamics of membrane proteins of Chinese hamster fibroblasts, *Cell Biol. Int.* **23**, 5, 345–350 (1999).
58. V. M. Mazhul', T. S. Chernovets, E. M. Zaitseva, D. G. Shcherbin, Action of serine proteases on intramolecular dynamics of membrane proteins of human platelets, *Biophysics* **47**(4), 607–616 (2002).



59. T. S. Chernovets, V. M. Mazhul', Role of protease-induced changes of internal dynamics of platelets membrane proteins in the intracellular signaling, in *28<sup>th</sup> Meeting of the federation of European biochemical societies* (Istanbul, 2002), *FEBS J.* p. 54.
60. V. Mazhul', T. Chernovets, E. Zaitseva, D. Shcherbin, Slow internal dynamics of membrane proteins in mechanisms of protease-induced aggregation of platelets, *Cell Biol. Int.* **27**, 571–578 (2003).
61. V. M. Mazhul', S. V. Konev, E. S. Lobanok, V. I. Levin, Phosphorescence analysis of structural-dynamics state of membrane proteins in the interaction of HLA-antibodies with determinants of lymphocytes receptors, *Dokl. Acad. Nauk BSSR* **41**(5), 69–72 (1997).
62. V. M. Mazhul', G. P. Matveikov, S. V. Konev, E. S. Kaliya, E. S. Lobanok, Reset of the structure-functional state of peripheral blood lymphocytes membranes of patients with CKB и PA, *Rheumatology* **6**, 103–107 (1992).
63. V. M. Mazhul', L. N. Kalituho, E. M. Zaitseva, J. V. Ivin, Brassinosteroides action to the structural-dynamics state of membrane proteins or plant cells, in *Abstracts of 5<sup>th</sup> international conference "Regulators of the grows and development of the plant"* (Moscow, 1999) pp. 113–114.
64. V. M. Mazhul', D. G. Shcherbin, E. M. Zaitseva, L. N. Kalituho, L. F. Kabashnicova, Tryptophan phosphorescence at room temperature of plants rootage, *Dokl. Acad. Nauk BSSR* **46**(2), 84–87 (2002).
65. V. M. Mazhul', L. S. Ivashkevich, D. G. Shcherbin, N. A. Pavlovskaya, G. V. Naumova, T. F. Ovchinnikova, Luminescence properties of humic substances, *J. Appl. Spectrosc.* **64**(4), 503–508 (1997).
66. V. M. Mazhul', D. G. Shcherbin, Low-temperature phosphorescence of lipid peroxidation products, *Biophysics* **43**(3), 431–437 (1998).
67. D. M. Gilligan, V. Bennett, The junctional complex of the membrane skeleton, *Semin. Hematol.* **30**, 74–83 (1993).
68. V. Bennett, A. J. Baines, Spectrin and ankyrin-based pathways: Metazoan inventions for integrating cells into tissues, *Physiol. Rev.* **81**, 1353–1392 (2001).
69. L. A. Sung, C. Vera, Protofilament and hexagon: A three-dimensional mechanical model for the junctional complex in the erythrocyte membrane skeleton, *Ann. Biomed. Eng.* **31**, 1314–1326 (2003).
70. G. T. Dodge, C. Mitchell, D. J. Hanahan, The preparation and chemical characteristics of hemoglobin-free ghosts of erythrocytes, *Arch. Biochim. Biophys.* **100**, 119–130 (1963).
71. V. Bennett, Proteins involved in membrane-cytoskeleton association in human erythrocytes: Spectrin, ankyrin, band 3, *Meth. Enzymol.* **96**, 313–324 (1983).
72. U. K. Laemmly, Cleavage of structural proteins during the assembly of the head of bacteriophage T4, *Nature* **227**, 680–685 (1970).
73. A. M. Kazennov, M. N. Maslova, A. D. Shagabodov, Role of membrane skeleton of erythrocytes in the functioning of membrane enzymes, *Dokl. Acad. Nauk BSSR* **312**(1), 223–226 (1990).
74. M. Maire, P. Champeil, J. V. Moller, Interaction of membrane proteins and lipids with solubilizing detergents, *Biochim. Biophys. Acta* **1508**, 86–111 (2000).
75. G. S. Menzies, K. Howland, M. T. Rae, T. A. Bramley, Stimulation of specific binding of [3H]-progesterone to bovine luteal cell-surface membranes: Specificity of digitonin, *Mol. Cell. Endocrinol.* **153**, 57–69 (1999).
76. M. Eilers, A. B. Patel, Comparison of helix interactions in membrane and soluble  $\alpha$ -bundle proteins, *Biophys. J.* **82**(5), 2720–2736 (2002).
77. M. Olivella, X. Deupi, C. Govaerts, Influence of the environment in the conformation of  $\alpha$ -helices studied by protein database search and molecular dynamics simulations, *Biophys. J.* **82**(6), 3207–3213 (2002).
78. A. Pusztai, S. Bardocz, S. W. Ewen, Uses of plant lectins in bioscience and biomedicine, *Front. Biosci.* **13**, 1130–1140 (2008).

79. H. Berman, K. Henrick, H. Nakamura, J. L. Markley, The worldwide Protein Data Bank (wwPDB): Ensuring a single, uniform archive of PDB data, *Nucleic Acids Res.* **35**, D301–D303 (2007).
80. R. A. Sayle, E. J. Milner-White, RasMol: Biomolecular graphics for all, *Trends Biochem. Sci.* **20**(9), 347–376 (1995).
81. J. H. Naismith, C. Emmerich, J. Habash, S. J. Harrop, J. R. Helliwell, W. N. Hunter, J. Raftery, A. J. Kalb, J. Yariv, Refined structure of Concanavalin-A complexed with methyl  $\alpha$ -D-mannopyranoside at 2.0 Angstrom resolution and comparison with the saccharide-free structure, *Acta Crystallogr. D. Biol. Crystallogr.* **50**, 847 (1994).
82. T. W. Hamelryck, M. H. Dao-Thi, F. Poortmans, M. J. Chrispeels, L. Wyns, R. Loris, The crystallographic structure of phytohemagglutinin, *J. Biol. Chem.* **271**, 20479 (1996).
83. C. S. Wright, Angstroms resolution structure analysis of two refined N-acetylneuraminyllactose – wheat germ agglutinin isolectin complexes, *J. Mol. Biol.* **215**, 635 (1990).
84. R. Ravishankar, K. Suguna, A. Surolia, M. Vijayan, Conformation, protein-carbohydrate interactions and a novel subunit association in the refined structure of peanut lectin-lactose complex, *J. Mol. Biol.* **259**, 281 (1996).
85. T. Prasthofer, S. R. Phillips, F. L. Suddath, J. A. Engler, Design, expression, and crystallization of recombinant lectin from the garden pea (*Pisum sativum*), *J. Biol. Chem.* **264**, 6793 (1989).
86. J. B. A. Ross, W. R. Laws, K. W. Roussland, H. R. Wyssbrod, Tyrosine fluorescence and phosphorescence from proteins and polypeptides, in *Topics in fluorescence spectroscopy*, Vol. **3**, edited by J. R. Lakowicz (Plenum Press, New York, 1992) pp. 1–63.
87. V. M. Mazhul', D. G. Shcherbin. Phosphorescence of lipid peroxidation products in solution and biological membranes, in *Spectroscopy of biological molecules*, edited by J. C. Merlin (Kluwer Academic Publishers, Dordrecht, 1995) pp. 401–402.
88. V. M. Mazhul', D. G. Shcherbin, Room temperature phosphorescence of intrinsic lipid chromophores in erythrocyte membranes, *Curr. Top. Biophys.* **22**(B), 138–142 (1998).
89. V. M. Mazhul', D. G. Shcherbin, Phosphorescence analysis of lipid peroxidation products in liposomes, *Biophysics* **44**(4), 656–661 (1999).
90. V. M. Mazhul', D. G. Shcherbin. Phosphorescent analysis of lipid peroxidation products in vitro and in situ, in *Spectroscopy of biological molecules: New directions*, edited by J. Greve, G. J. Puppels, C. Otto, (Kluwer Academic Publishers, Dordrecht, 1999) pp. 349–350.
91. V. M. Mazhul', D. G. Shcherbin, The heterogeneity of development of lipid peroxidation process in bulk and annular lipids of biological membranes, *Curr. Top. Biophys.* **24**(2), 139–146 (2000).